Journal of King Saud University – Science 35 (2023) 102716

HOSTED BY

Contents lists available at ScienceDirect

Journal of King Saud University – Science

journal homepage: www.sciencedirect.com

Original article

Targeting JAK/STAT signaling pathway and anti-inflammatory markers using bakuchiol isolated from *Psoralea corylifolia* for cytotoxicity of human squamous cell carcinoma (A431) cells

Shivani Attri [a], Atamjit Singh [b], Farhana Rashid [a], Sharabjit Singh [a], Pallvi Mohana [a], Sameer Alshehri [c], Atiah H. Almalki [d,e], Ales Pavlik [f], Shafiul Haque [g,h,i], Ajay Kumar [j], Saroj Arora [a,*]

[a] *Department of Botanical & Environmental Sciences, Guru Nanak Dev University, Amritsar, Punjab, India*
[b] *Department of Pharmaceutical Sciences, Guru Nanak Dev University, Amritsar, Punjab, India*
[c] *Department of Pharmaceutics and Industrial Pharmacy, College of Pharmacy, Taif University, P.O. Box 11099, Taif 21944, Saudi Arabia*
[d] *Department of Pharmaceutical Chemistry, College of Pharmacy, Taif University, P.O. Box 11099, Taif 21944, Saudi Arabia*
[e] *Addiction and Neuroscience Research Unit, College of Pharmacy, Taif University, Al-Hawiah, Taif 21944, Saudi Arabia*
[f] *Laboratory of Animal Physiology, Department of Animal Morphology, Physiology and Genetics, Faculty of AgriSciences, Mendel University in Brno, Zemedelska1, 61300 Brno, Czech Republic*
[g] *Research and Scientific Studies Unit, College of Nursing and Allied Health Sciences, Jazan University, Jazan 45142, Saudi Arabia*
[h] *Gilbert and Rose-Marie Chagoury School of Medicine, Lebanese American University, Beirut, Lebanon*
[i] *Centre of Medical and Bio-Allied Health Sciences Research, Ajman University, Ajman, United Arab Emirates*
[j] *University Centre for Research & Development, University Institute of Pharmaceutical Sciences, Chandigarh University, Gharuan, Mohali, Punjab, India*

ARTICLE INFO

Article history:
Received 26 September 2022
Revised 7 May 2023
Accepted 11 May 2023
Available online 18 May 2023

Keywords:
Antiproliferative activity
Apoptosis induction
Psoralea corylifolia
Squamous
Reactive oxygen species

ABSTRACT

Objectives: Non melanoma skin cancers are common neoplasms worldwide. In India, squamous cell carcinoma (SCC), is the most prevalent skin disorder and its incidence rises quickly with cumulative exposure to sun. Numerous techniques are available for SCC but reversion and metastasis are common concern that needs effective and safe strategies for its control. With this in view, the study was planned to investigate the activity of Bakuchiol (Bak), traditionally used in various countries for curing skin ailments but its mechanism of action is unexplored. In our study, we explored anti-proliferative, pro-apoptotic and anti-inflammatory potential of Bak toward human squamous carcinoma (A431) cell line.
Methods: The pure compound Bak was isolated from the plant *Psoralea corylifolia* and characterized using NMR, HRMS and FTIR. To explore their bioefficacy, different *in vitro* assays were performed against A431 cell line. To have molecular insights, RT-qPCR investigation was done to analyzed the expression level of inflammatory markers (TLR 9, IFN β, IL 23, JAK 3 and STAT 3).
Results: The results showed the growth inhibitory effect on A431 cells after Bak treatment in dose-dependent way. To understand mode of cell death, cells were initially analyzed under phase-contrast, fluorescence and scanning electron microscope that showed characteristics of apoptosis. Furthermore, cell cycle studies with a flow cytometer were carried out which showed increased level of ROS, reduced MMP and cells arrested at G_0/G_1 phase in Bak treated cells further strengthening the induction of apoptosis. Moreover, RT-qPCR analysis indicated the downregulation of inflammatory markers in Bak-treated A431 cells that further confirmed its therapeutic role. The molecular docking study also confirmed that Bak has perfect scaffold that can complete the pharmacophoric need for JAK3 kinase inhibition.

Abbreviations: AO/EtBr, Acridine orange/ethidium bromide; A431, Skin epidermoid carcinoma cells; DMEM, Dulbecco's modified Eagle's medium; DCFH-DA, 2,7-dichlorofluorescein diacetate; EA, Early apoptosis; FTIR, Fourier-transform infrared spectroscopy; FBS, Fetal bovine serum; HeLa, Human cervical cancer; HRMS, High resolution mass spectrometry; IL, Interleukin; IFN, Interferons; JAK, Janus kinase; LA, Late apoptosis; L, live; L929, Human fibroblast; MTT, 3-(4,5-dimethylthiazol-2-yl)-2,5-diphenylte-trazolium bromide; MG-63, Human osteosarcoma; MEM, Minimal essential media; MMP, Mitochondrial membrane potential; NCCS, National Centre for Cell Science; NMR, Nuclear magnetic resonance; PI, Propidium iodide; Rh123, Rhodamine123; RT-qPCR, Quantitative real-time polymerase chain reaction; ROS, Reactive oxygen species; STAT, Signal transducer and activator of transcription TLR, Toll-like receptor.

* Corresponding author at: Department of Botanical & Environmental Sciences, Guru Nanak Dev University, Amritsar 143005, Punjab, India.

Peer review under responsibility of King Saud University. Production and hosting by Elsevier.

Production and hosting by Elsevier

https://doi.org/10.1016/j.jksus.2023.102716

Conclusion: A critical analysis of results points towards the role of Bak in ameliorating inflammatory markers along with apoptosis induction in A431 cells by regulating the expression level of variable markers.

1. Introduction

The uncontrolled proliferation and division of mutated cells lead to a deadly disease called Cancer. According to World Health Organization (WHO), approximately 14 million cancer cases along with 8.2 million mortalities reported because of cancer (Grace Nirmala et al., 2018). In the United States, the most widely identified skin cancers are melanoma and nonmelanoma (NMSC) (Leiter and Garbe, 2008). In early stages, NMSC is readily detectable, limited malignancy and has low mortality with respect to other cancers. Basal cell carcinoma (BCC) and squamous cell carcinoma (SCC) are the most common groups of NMSC (Barton et al., 2017). BCC is the form that constitutes up 80% of skin cancer and initiates in basal cells of the epidermis layer whereas SCC rises in the squamous layer of epidermis and constitutes 16% of skin cancers. Although, BCCs are not life-threatening, if remain untreated, they cause local ulceration, loss of basic function and deformity. In contrast, SCC causes major morbidity and mortality worldwide due to its invasiveness and metastasis potential (Chamcheu et al., 2018). In India, among all types of cancer, skin cancer accounts 1–2%, with several studies revealing that SCC is the most prevalent skin malignancy as compared to BCC within dark-skinned individuals (Panda, 2010). Histologically, SCC is a different kind of malignancy that develops through an uncontrollable proliferation of epithelial cells or cells that exhibit cytological or tissue architectural features of stem cell differentiation such as occurrence of keratin, bundles of tonofilament or desmosomes, which are structures that participate in cell-to-cell adhesion. Among all reports of SCC, 2.5% are metastatic which leads to significant morbidity resulting an extensive economic burden on the healthcare system. Although the skin gets exposed to several carcinogens and mutagens, ultraviolet exposure is the major cause of SCC development (Yan et al., 2011). The damage in dermal cells might be directed by exposure to UV radiations or indirectly by UV-induced overproduction of ROS (Reactive oxygen species) which ultimately induce oxidative stress in the skin. This ultimately leads to single and double-strand breaks in DNA, misexpression and activates the cascade of skin carcinogenesis (Xian et al., 2019). The generation of ROS along with oxidative stress initiates the cascade of signaling pathways which involves the development of cancer by modulating proliferation, invasion, angiogenesis, metastasis and inflammation (Vallée and Lecarpentier, 2018). Over the last few decades, there is an increase in the cases of SCC worldwide. Therefore, an urgent need for understanding the molecular pathways and gene networks linked with the development of skin carcinoma.

Now, it is widely accepted that continuing inflammation, innate immunity and tumor have a close relationship and comparisons in the modulatory pathways have been considered for more than a century. While cell progression alone is not responsible to initiate cancer, a continuous proliferation of cells in surrounding rich in inflammatory cells, hormones, active stroma and DNA damage-promoting cytokines undoubtedly promote tumor growth. Interleukins possess a valuable role in inflammation associated with tumor growth and development. The signaling cascade of IL-23 is well documented and involves various downstream signal markers including Janus associated kinase 2 (Jak2) and Toll-like receptors (TLRs). TLRs, a family of molecules that recognize conserved pathogen-associated molecular patterns (PAMPs) and are expressed in tumor microenvironment (TME) serve as an important marker to induce innate immune system. Despite the initiation of self-programmed death, TLRs also initiate the release of cytokines and recruit further immune cells to secrete pro-inflammatory cytokines and growth factors which might restore anti-cancer purpose of APCs (Antigen-presenting cells) and effector T-cells. This unsuitable increment of immune cells functions and anti-tumor immune via TLRs network will serve as signal to modulate cancer progression, division, reversion and acceptance of chemotherapy (Cen et al., 2018).

Although the number of conventional therapies are known for the management of NMSC including surgical removal, topical and systemic drug therapies. Currently, numerous drugs are available for regulating skin cancer including doxorubicin, vincristine, cisplatin, 5-fluorouracil and bleomycin but these drugs lack specificity in their action (Vijaybabu and Punnagai, 2019). So, there is a keen interest in developing alternative and safe therapies especially prepared from medicinal plants. Botanicals are proven to be a safe, effective, non-invasive and cheap remedy for curing variable diseases including cancer. These botanicals posseses multiple properties such as immunomodulatory, anti-inflammatory, antioxidant and anticancer and prove to be a therapeutic approach to inhibit or reverse the process of carcinogenesis. *Psoralea corylifolia* (babchi), a medicinal plant of family fabaceae used conventionally in Ayurvedic and Chinese medicine due to its magical effects to improve numerous skin diseases like psoriasis, vitiligo, eczema, leprosy and other maladies. Bakuchiol (Bak) is one of the key components of *P. corylifolia,* a meroterpene with resveratrol-like structure and used as a cosmetic ingredient due to its antioxidant, antifungal, antibacterial, anti-wrinkling and pro-apoptotic potential (Khushboo et al., 2010). Bak also possesses anticancer and anti-inflammatory activities. According to the literature, Bak showed anti-cancer effects via inhibiting proliferation of breast, lung, skin and colon cancer cell lines (Jafernik et al., 2021). Hence, Bak may be promising chemopreventive/chemotherapeutic approach, particularly for skin malignancy. However, impact of Bak on skin cancer and associated molecular/signaling cascade has not been entirely explored. In our research work, we analyzed effect of Bak on proliferation of cells and its death-inducing potential in squamous carcinoma A431 cells and determined whether JAK 3, STAT 3, IL-23, IFN β and TLR 9 receptors were involved to attenuate skin carcinogenesis.

2. Methodology and materials

2.1. Chemicals and reagents

The solvent hexane was used for extraction from the seeds of *P. corylifolia* and Fetal Bovine Serum (FBS), Rhodamine-123, Hoechst 33342, Fluoromount and 2′,7′- Dichlorodihydrofluorescein diacetate (DCFH-DA) were procured from the sigma chemicals (USA). Trypsin, 3-(4,5-dimethylthiazol-2-yl)-2,5-diphenyl tetrazolium bromide (MTT) and Minimal essential medium (MEM) were bought from Hi-media, Mumbai (India). The additional analytical (AR) grade chemicals and reagents utilized in investigations.

2.2. Procurement and authentication of plant material

The plant *P. corylifolia* (seeds) were purchased from Amritsar in May 2019 and identified by the Herbal Health Research Consortium (HHRC) Pvt. Ltd. Amritsar, Punjab (India) is affiliated with the National Medicinal Plant Board (NMPB), Government of India and has the accession number RS 155. A voucher specimen with reference number (962). has been submitted to the herbarium lab of the Department of Botanical and Environmental Sciences, GNDU, Amritsar, India.

2.3. Extraction and fractionation

The seeds of *P. corylifolia* were cleaned with distilled water and dried in an oven at 40 °C. The seeds were ground to coarse powder and macerated in 80% methanol and then sequential extraction was done with other solvents *viz*, hexane (PcH), chloroform (PcC), ethyl acetate (PcE), n-butanol (PcB) and aqueous (PcA) fraction. Each fraction was sieved by Whatman paper, then evaporated to dryness through rotavapor. Each of the dried fractions/extract was stored at 4 °C and reconstituted in DMSO (0.1%) for further experiments.

2.4. Column chromatography of hexane fraction (PcH) of Psoralea corylifolia

2.4.1. Isolation of bakuchiol

The fraction *PcH* (3 g) of *P. corylifolia* poured in a glass column packed by silica with mesh size 60–120 using *n*-hexane solvent. The proportion of solvent *n*-hexane (Hex): ethyl acetate (EtAc) used as eluent to obtain the target compound. Using the pure hexane solvent, total 300 fractions of 50 ml each were taken. Then, analyzed on TLC (Thin layer chromatography), a blue color fluorescent single spot was observed and concentrated. The isolated compound was named Bakuchiol (Bak) (100 mg) after characterized through different spectroscopic techniques.

2.4.2. Structure elucidation and characterization of bakuchiol

2.4.2.1. ^{1}H and ^{13}C NMR spectra. ^{1}H and ^{13}C NMR spectra of Bak (10 mg/ml) was analyzed on 500 MHz Bruker NMR instrument using solvent $CDCl_3$. The chemical shift (ppm) was analyzed with respect to Tetrametysilane (TMS) as reference compound and coupling constant *J*, was taken in Hz, multiplicity is represented as: s = singlet, d = doublet, t = triplet, m = multiplets.

2.4.2.2. FTIR. FTIR spectra of isolated compound Bak was recorded with Agilent-FTIR technologies, USA, FTIR Spectrophotometer which identify the presence of organic molecular groups, functional groups and cross-links involved and showed characteristic vibrational frequencies in the infra-red range. A compound in the form of powder was used for analysis in FTIR.

2.4.2.3. Mass spectroscopy (HRMS). The compound was dissolved in the ratio of 1:1 (acetonitrile: water HPLC grade) and sonicated at room temperature for 30 min for proper mixing. The spectrum (fragmentation pattern) was then recorded when 20 µl of the solution was put into the capillary tube of the mass spectrophotometer (LC-MS/MS spectrometer, HRMS Bruker, Massachusetts).

2.5. Cell culture

2.5.1. Procurement and maintenance of cancer cell lines

A human squamous cell carcinoma (A431) cell line, human osteosarcoma (MG-63) cell line, human cervical cancer (HeLa) cell line and normal human fibroblast (L929) cell lines were used in this study and these cell lines were procured from the National Centre for Cell Science (NCCS) Pune, India. The cells were regularly maintained in MEM and DMEM along with 10% FBS, antibiotic–antimycotic solution according to respective cell lines and incubated in the humified environment at 37 °C with 5% CO_2.

2.5.2. Composition of MEM and DMEM medium

The MEM medium used for the A431 cell line purchased from the Himedia (RSL008G) consist of Minimum Essential Medium Eagle with Earle's salts, L-alanyl-L-glutamine, NEAA and sodium bicarbonate. Moreover, 10% FBS and antibiotic-antimycotic solution also added in the prepared medium. Furthermore, the DMEM medium per 100 ml solution containing DMEM (1.0 g), Sodium bicarbonate (0.37 g), Streptomycin (10.0 mg), Penicillin (6.4 mg), Gentamycin (100 µl), FBS (10.0 ml).

2.5.3. Measurement of cytotoxicity

To analyzed the cytotoxicity of isolated compound, MTT assay was used as per method suggested by Kumar et al., (2021) along minute alterations. Cells (8×10^3 cells/100 µl) were injected into 96-well plates until confluency. The confluent cells were allowed to treat with serial doses (6.09, 12.18, 24.3, 48.5, 97.5, 195 µM) of Bak for 24 h. After treatment of 24 h, MTT (20 µl) was poured into every well and allow to incubate for 4 h. Afterwards, supernatant was discarded from the plate and DMSO with volume of 100 µl was injected into every well for dissolving crystals of formazan. At last, reading was recorded (570 nm) by multimode ELISA reader.

$$Inhibition(\%) = \frac{A_c - A_s}{A_c} \times 100$$

Where, Absorbance of control, A_c.
Absorbance of sample, A_s.

2.6. Detection of apoptosis by cell morphological assessment

The alterations in the cell morphology were analyzed using phase-contrast microscopy, fluorescence and scanning electron microscope (SEM) after given treatment of Bak to human squamous carcinoma A431 cells. All studies related to apoptosis were done by seeding (2×10^5) A431 cells into 24-well plates along coverslips in every well. The confluent cells after 24 h, were treated with increasing doses (IC_{30}: 2.10 µM/ml; IC_{50}: 9.06 µM/ml and IC_{70}: 38.88 µM/ml) of Bak and analyzed as described under the following subsections.

2.6.1. Phase-contrast microscopy

To observe the alterations in morphology of A431 cells, the cells (2×10^5/well) were plated in 24-well plate along with coverslips (12 mm) in every well for 24 h. After confluency, Bak treatment with increasing concentrations were given for 24 h and then slides were seen underneath phase-contrast microscope.

2.6.2. Scanning electron microscopy (SEM)

Measurement of Bak effect on A431 cells, both treated as well as untreated cells were examined under SEM as according to the procedure proposed by Ramasamy et al., (2022) with minor changes. Cells (2×10^5/well) were poured into 24-well plates in each well with coverslips at base. After confluency, the treatment of Bak was given to the cells. The cells were fixed using 4% paraformaldehyde (PFA) and 2.5% glutaraldehyde and kept at −20°C for 4 h. Then, dehydration was done with series of cooled ethanol for 5 min each. After that, on aluminium metal stubs where double-sided tape was fixed, the coverslips were placed on it followed by sputter-coater using silver (Quorum Q150R ES). The cell images were collected with scanning electron microscope.

2.7. Fluorescence microscopy

2.7.1. Hoechst 33,342 staining

The morphological alterations in the nucleus induced by the Bak treatment were analyzed by Hoechst 33,342 stain according to protocol proposed by Yadav et al., (2017) with little modifications. Cells with density 2×10^5/well were plated into 24-well plates along with clean coverslips. Followed by 24 h, the treatment with increasing concentrations of Bak were given to cells. The washing was given to cells with 1x PBS followed by fixation using 4% paraformaldehyde (PFA) for 15–20 min and again given washing using PBS. After that, 3 µl Hoechst 33,342 (10 µg/ml) dye was poured to stain cells with incubation for 30 min in dark followed by thrice washing using PBS. Then, coverslips were mounted onto slides using drop of flouramount and images were taken under fluorescence microscope at a magnification of 10X.

2.7.2. Acridine orange (AO) and ethidium bromide (EtBr) staining

To examine cascade of apoptosis and changes in nucleus through apoptosis in A431 cells, we used acridine orange/ethidium bromide (AO/EtBr) stain as procedure adopted by Fattahi et al., (2013) with few changes. A431 cells (2×10^5/well) were treated with Bak (2.10 µM/ml; 9.06 µM/ml; 38.88 µM/ml) and incubate for 24 h. Then, both floating and attached cells were pooled and centrifuged to form a pellet at 2500 rpm for 5 min. The obtained cell pellet was resuspended in 1 × PBS (100 µl) and incubated with 5 µl AO/EtBr mixture (60 µg/ml AO and 100 µg/ml EtBr, both prepared in PBS) for 5 min. After that, stained cell mixture (25 µl) was plated on clean slide, immediately placed a coverslip on it and observed using fluorescence microscope. The differential AO/EtBr staining has the potential to distinguish viable and non-viable cells depend upon membrane integrity. AO introduces into DNA and gives a green color in case of viable cells but after intercalation of EtBr into DNA, nonviable cells appear orange in color.

2.7.3. Rhodamine 123 (Rh-123) staining

To examine the effect of Bak on mitochondrial membrane potential in A431 cell line, Rh-123 stain was used as protocol suggested by Kumar et al., (2021) with some alterations. Cells at density 2×10^5/well were plated into 24-well plates till confluency followed by treatment with increasing doses of Bak. After 24 h of treatment, cells were allowed to wash using 1x PBS and fixed by 4% paraformaldehyde for 15–20 min. Afterwards, again washing was done using PBS and 1 µl of Rh-123 solution (2 µg/ml) was poured into cells, incubated for 30 min in CO_2 incubator. To remove the complete traces of dye, thrice washed with PBS and using fluorescence microscope images were taken.

2.8. Flow cytometric studies

2.8.1. Analysis of accumulated ROS (Reactive oxygen species)

To analyzed production of reactive oxygen species in A431 cells, flow cytometry with DCFH2-DA probe was used by adopting procedure suggested by Kumar et al., (2014) with some modifications. DCFH-DA is a non-polar stable constituent which easily permeable inside cells and hydrolyzed via enzyme esterase to produce 2′,7′ dichlorodihydrofluorescin (DCFH2). The generation of hydrogen or low molecular weight peroxides by the cells results a more fluorescent 2′,7′-dichlorofluorescein (DCF) compound by oxidizing DCFH2 (Afri et al., 2004). Thus, the intensity of fluorescence depended upon the produced hydrogen peroxide by the cells. A431 cells at density 4×10^5 cells/well were cultivated into 24-well plate and allowed to treated with Bak. After 24 h, cells were incubated using stain (10 µM) at 37°C in the dark for 30 min, then collection and washing of cells was done using 1x PBS. The generated ROS stress in cells was examined by Flow Cytometer.

2.8.2. Analysis of MMP ($\Delta\Psi m$) (Mitochondrial membrane potential)

The loss of *MMP* ($\Delta\Psi m$) was analyzed in A431 cells using fluorescent indicator Rh123 measured by flow cytometry as per the protocol suggested by Tian and Zang, (2015) with few amendments. Briefly, cells (4×10^5 cells/well) seeded into 24-well plate till confluency. Afterward, the treatment of Bak (2.10 µM/ml; 9.06 µM/ml; 38.88 µM/ml) was given to cells. Then, cells were given washing with PBS followed by staining using rhodamine123 (5 µg/ml) in dark at 37°C for 30 min. Then, cells were allowed to washed, trypsinized and centrifuged to form a pellet. The collected pellet was resuspended in 1x PBS to analyze the fluorescence of cells using flow cytometer.

2.8.3. CellCycle phase distribution analysis

To analyze the effect of Bak on relative content of cellular DNA, cell cycle analysis was done on A431 cells using flow cytometry as per procedure suggested by Kumar et al., (2021) along some changes. Cells at density 4×10^5 cells/well were seeded into 24-well plates and treated with IC_{30} (2.10 µM/ml), IC_{50} (9.06 µM/ml) and IC_{70} (38.88 µM/ml) doses of Bak. Afterward, given washing to cells with PBS and stained using propidium iodide (10 µg/ml) and incubate for 30 min in dark at room temperature. Untreated cells measured simultaneously, considered as negative control. The DNA content of apoptotic cells were measured by quantifying the phase of the cell cycle using Flow Cytometer.

2.8.4. Apoptosis assay using Annexin V-FITC

To examine the cell death enhancing potentcy of Bak in A431 cells, Annexin V-FITC Apoptosis Detection Kit (Sigma) was used as per protocol proposed by Al-Oqail et al., (2021) with some changes. Briefly, cells (4×10^5 cells/well) were seeded into 24-well plate for 24 h and treated with IC_{30} (2.10 µM/ml), IC_{50} (9.06 µM/ml) and IC_{70} (38.88 µM/ml) concentration of Bak. Following treatments, cells were collected and centrifuged to form a pellet. Thereafter, control and exposed cell pellet were resuspended in buffer and stained with Annexin V-FITC (5 µl) and propidium iodide (10 µl) to cell suspension and incubate for 10 min in dark. Using flow cytometer, population of apoptotic and necrotic cells were examined.

2.9. Quantitative Real-time polymerase chain reaction (RT-qPCR)

RNA from untreated and treated A431 cells was extracted using Trizol reagent as per manufacturer procedure. Cells were given a treatment of Bak for 24 h, then given washing with chilled PBS. The RNA samples were allowed to mix in TE buffer and kept at 60 °C for 5 min. Next, to eliminate DNA contamination, DNase I was used with incubation for 30 min at 37 °C. Thereafter, absorbance of RNA was taken using Nano-Drop spectrophotometer at 260 nm and 280 nm. Afterward, cDNA was synthesized in a final reaction volume by taking similar concentrations of RNA through iScriptTM cDNA kit as per the suggested protocol. Then, quantified synthesized cDNA and equal concentration was used to accomplish RT-qPCR using iQSYBRSupermix system. In this study, TLR 9, IFN β, IL 23, JAK 3 and STAT 3 primer sequences were utilized and obtained from NCBI (National Center for Biotechnology Information) gene bank database are shown in Table 1. The reaction of RT-qPCR was performed on Applied Biosystems to observe the relative gene expression. By using comparative threshold cycle method (ΔΔCT), the expression of every gene was calculated. β-actin was taken as a control. The resultant Ct value of each gene was neutralized by Ct value of β-actin. Then, expressions of each gene was represented as $2^{-\Delta\Delta Ct} \pm$ SE.

Table 1
RT-PCR primers sequence analysis.

S. No.	Primer Name	Accession No.	Product Size	Oligonucleotides (5′-3′) sequence	Source
1.	TLR 9	NM_017442.4	144	Forward-CGTGGTCTTCGACAAAACGC Reverse - GAGGTTTACAGGTTCTCAAA	NCBI
2.	IL 23	NM_016584.3	162	Forward- CTCGCTCCCTGATAGCCCT Reverse- TGCGAAGGTTTTGAAGCGG	NCBI
3.	IFN β	NM_002176.4	173	Forward- TAGGCGACACTGTTCGTGTT Reverse- CCATTCAATTGCCACAGGAGC	NCBI
4.	JAK 3	NM_001320923.2	108	Forward- TCGTGATGGGCTGTGGAATG Reverse- CTGTATTGTCGCCTAGCGGG	NCBI
5.	STAT 3	NM_006099.3	119	Forward- TGATGAGTTTCCGGGTGTCTG Reverse- AAGCGTCGTCGGTAAAGCTC	NCBI
6.	β-actin	T25383	166	Forward- GTCCTCTCCCAAGTCACACA Reverse-GCTCATACATCTCAAGTTGGGAC	NCBI

2.10. Molecular docking studies

The crystal structure of JAK3 kinase in complex with its inhibitor 9YV (PDB entry: 5 W86; Resolution: 2.61 Å) was retrieved from Protein Data Bank (https://www.rcsb.org/structure/5w86). The preparation of structures was done using the drug design platform LeadIT [LeadIT version 2.3.2]. Co-crystalized ligand 9YV was taken to examine the binding site in JAK3 kinase with radius of 6.50 Å. Using ChemDraw Ultra (2013), the structure of Bak was drawn and its energy was lowered using MM2 force field in Chem3D Ultra software (Cambridge, USA) (ChemDraw Ultra 6.0 and Chem3D Ultra). The prepared Bak structure was taken as protonated in aqueous solution and docked into organized binding location of JAK3 kinase through the FlexX docking module in LeadIT. All FlexX solutions yielded were recorded by a consensus scoring function (CScore) and numbered accordingly. The top best pose with the maximum score was taken for the analysis of interactions. using Discovery Studio Visualizer (Dassault Systemes BIOVIA, 2017), 3D interactions were visualized.

2.11. Statistical analysis

To examine the significance difference between all the values, One-way ANOVA (Analysis of Variance) was used. Further, high-range statistical domain (HSD) using Tukey's test was used to compared the difference between the means. All values were represented as Mean ± standard errors (SE). The probability $p \leq 0.05$ was used to examined that all the values were statistically significant at 5% level of significance.

3. Results

3.1. Isolation and identification of potent compound

3.1.1. Pure compound isolation using column chromatography

Bak was obtained from fraction *PcH* of *P. corylifolia* using silica gel column chromatography which showed a blue color spot on thin layer chromatographic plates when seen under UV light.

3.1.2. Characterization of Bak using spectroscopic techniques

Bak was obtained from fraction *PcH* of *Psoralea corylifolia. Bak* structure was confirmed using NMR and IR techniques (Fig. 1). In spectrum of ^{1}H NMR, (500 MHz, DMSO d_6) δ 7.245–7.228 (m, 2H), 6.769–6.752 (m, 2H), 6.263–6.230 (d, J = 16.5 Hz, 1H), 6.066–6.033 (d, J = 16.5 Hz, 1H), 5.904–5.847 (m, 1H), 5.125–5.090 (m, 1H), 5.043–4.989 (m, 2H), 1.975–1.927 (m, 2H), 1.67–1.68 (m, 3H), 1.578 (s, 3H), 1.506–1.472 (m, 2H), 1.190 (s, 3H) (Fig. S1). ^{13}C NMR (125 MHz, DMSO d_6) δ 154.68, 146.00, 135.87, 131.33, 130.89, 127.40, 126.52, 124.85, 115.42, 111.91, 42.55, 41.32, 25.72, 23.39, 17.67 (Fig. S2). In the FTIR spectrum the peak at 2914.8 to 2855.1 showed CH_3 stretching and peak at 3481.3 indicated OH group. The peak at 1610.2 to 1468.6 showed the aromatic C–H stretching and plane bending in C–H at 1244.9 whereas peak at 849.8 represent C–H bending (aromatic) (Fig. S3). Bak HRMS spectrum showed only peak at m/z 257.30 which represents the molecular formula to be $C_{18}H_{24}O$. (Fig. S4).

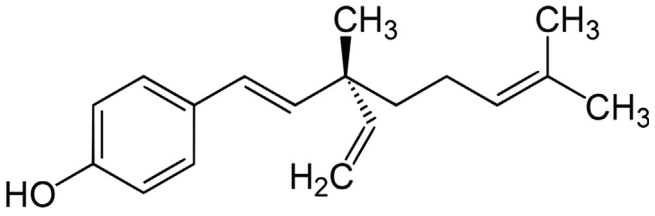

Fig. 1. The chemical structure of bakuchiol (4-[(1E,3S)-3-Ethenyl-3,7-dimethyl-locta-1,6-dien-1-yl] phenol.

3.2. Cytotoxicity of bakuchiol

The growth inhibitory effect of Bak was checked against the panel of cells viz. A431, MG-63, Hela and normal cell line L929. The antiproliferative potential of Bak was examined in a dose-dependent way. Bak possesses effective growth inhibitory effect with IC_{50} value of 9.06, 19.12 and 31.55 µM/ml towards A431, MG-63 and HeLa respectively. Growth inhibitory effect against L929 cell line is less possesses high IC_{50} value of 74.97 µM/ml. In MTT assay, Bak showed maximum cytotoxic potential against A431 cell line (Fig. 2 and Table 2).

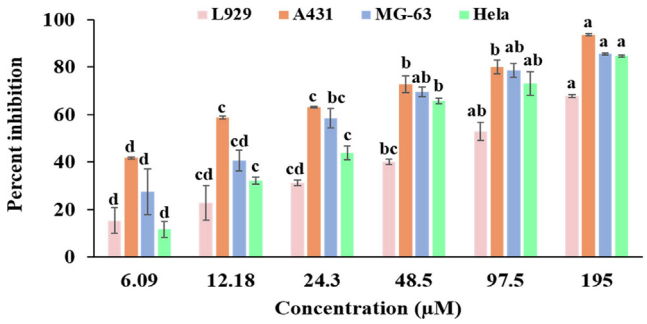

Fig. 2. Cell viability was determined using MTT assay. Cells were treated with varying concentrations (6.09, 12.18, 24.3, 48.5, 97.5, 195 µM) of bakuchiol obtained from *P. corylifolia* on A431, MG-63, HeLa and L929 cells for 24 h. Data represented as Mean ± SE. Data labels with different letters (a, b, c and d) represent significant difference among them at $p \leq 0.05$ level of significance.

Table 2
Cytotoxic effect of Bakuchiol from *P. corylifolia* on *A431*, *MG-63*, *HeLa* and *L929* cell lines in MTT assay.

Conc (µg/ml)	*L929*	*A431*	*MG-63*	*HeLa*
6.09	15.28 ± 5.48^{d}	41.73 ± 0.46^{d}	27.58 ± 9.62^{d}	11.59 ± 3.45^{d}
12.18	22.92 ± 7.28 ^{cd}	58.69 ± 0.61^{c}	40.59 ± 4.37 ^{cd}	32.15 ± 1.59^{c}
24.3	31.37 ± 1.12 ^{cd}	63.17 ± 0.28^{c}	58.47 ± 4.01^{bc}	43.83 ± 2.82^{c}
48.5	40.01 ± 1.08^{bc}	72.78 ± 3.56^{b}	69.48 ± 2.06^{ab}	65.76 ± 1.03^{b}
97.5	52.91 ± 3.92^{ab}	80.07 ± 3.03^{b}	78.61 ± 3.00^{ab}	73.01 ± 4.98^{ab}
195	67.86 ± 0.62^{a}	93.62 ± 0.44^{a}	85.55 ± 0.49^{a}	84.63 ± 0.49^{a}
IC_{50} (µg/ml)	74.97	9.06	19.12	31.55
Regression equation	y = 14.90ln(x) – 14.33	y = 13.28ln(x) + 30.15	y = 17.09ln(x) – 0.45	y = 21.00ln(x) – 22.49
Camptothecin (IC_{50}) (µM)	66.44	29.47	57.12	46.24
R^2	0.980	0.980	0.97	0.97
F-ratio	22.54**	85.61**	21.36**	93.62**
HSD	19.52	9.25	23.07	13.51

Significance level (**$p \leq 0.01$).
Values expressed as Mean ± SE. Means with different superscripts alphabets (a, b, c, d and e) represent significantly different values.

3.3. Alterations in A431 cell morphology

Bak showed antiproliferative potential towards human squamous carcinoma A431 cell line. Therefore, it was further examined whether its cytotoxic activity is linked to its capability to induce apoptosis in A431 cells. So, different microscopes (phase-contrast, fluorescence and Scanning electron microscope) were used to analyzed changes in cell integrity after treatment with IC_{30} (2.10 µM/ml), IC_{50} (9.06 µM/ml) and IC_{70} (38.88 µM/ml) value of Bak. The observations under phase-contrast microscope revealed that exposure of Bak to A431 cells showed typical apoptotic features such as detachment of cells from the substrate, shrinkage of cytoplasmic periphery and reduce volume of cells whereas the untreated A431 cells had intact morphology (attached, flattened and dense multilayer) (Fig. 3A) Such observations showed that Bak reduces A431 cells viability in concentration-dependent manner.

The structural changes examined under the scanning electron microscope (SEM) indicated that Bak has potential to initiate cell death in A431 cells. The images of SEM cells revealed apoptotic characteristics such as the decrease in size, condensed and rounding-off cells, appearance of membrane blebbing and apoptotic bodies, in a dose-dependent manner whereas control cells showed intact morphology without any deformity in A431 cells (Fig. 3B).

3.4. Apoptosis detection by Hoechst 33342, AO/EtBr, Rh-123

Cells examination under fluorescence microscope done by incubate the cells with Hoechst 33,342 and AO/EtBr stains. The

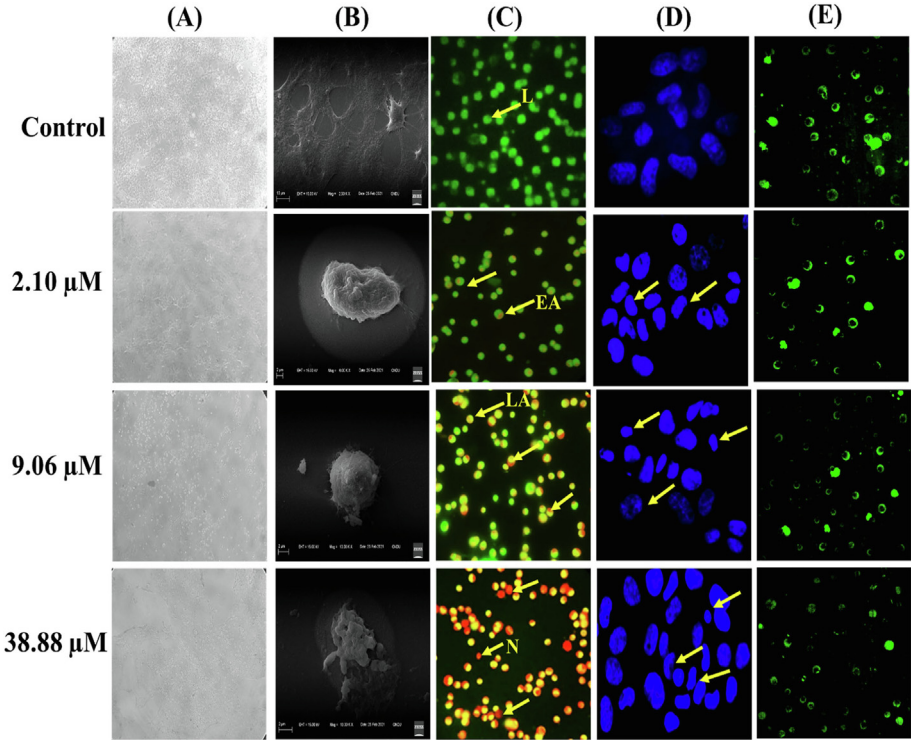

Fig. 3. (A) Brightfield images of A431 cell line **(B)** Scanning electron micrographs (SEM) images of A431 cells. **(C)** Fluorescence microscopic images of Acridine orange and ethidium bromide (AO/EtBr) staining of A431 cancer cell line. Arrow indicated live (L) cells; early apoptotic (EA); late apoptotic (LA) and necrotic (N) cells population. **(D)** A431 cells stained with Hoechst 33,342 dye visualized using a fluorescence microscope **(E)** A431 cells stained with Rhodamine 123 showing disruption of mitochondrial membrane potential.

microscopic observations showed that live cells (viable cells) having intact morphology, took up AO and fluorescence green in color. On treatment with different concentrations (2.10 μM/ml, 9.06 μM/ml and 38.88 μM/ml) of Bak, cells showed apoptotic features and altered cell morphology such as chromatin condensation, fragmentation and cellular shrink. Early apoptotic cells showed bright green nuclei and condensed orange-red nuclei were observed in late apoptotic cells as shown in (Fig. 3C). There was a significant increase in apoptotic cells with condensed and fragmented chromatin at the highest concentration. Furthermore, the number of necrotic cells with orange nuclei increased with an increased concentration of Bak. Taken together, these results conclude that Bak exhibits inhibitory activity towards squamous carcinoma A431 cell line via enhancing cell death through an apoptotic-mediated pathway. Hoechst 33,342 is a fluorescent DNA-binding dye that easily permeable into cells and insert into A-T region of the DNA (Bucevičius et al., 2018). The nuclei of cells after treatment with Bak showed a bright blue fluorescence and were smaller in size as compared to control. Therefore, on treatment with different doses (IC_{30}; 2.10 μM/ml, IC_{50}; 9.06 μM/ml and IC_{70}; 38.88 μM/ml) of Bak, there is nuclear fragmentation and condensation of chromatin or nuclei were examined, without any such alternations were observed in untreated cells as shown in Fig. 3D.

Further, the decrease in mitochondrial membrane potential (MMP/$\Delta\psi m$) is a key feature of cell death. It was stated that mitochondrial permeability transition pore (PTP) plays an essential role in apoptosis via releasing certain mitochondrial apoptogenic factors in some cell types (Wageesha et al., 2017). Mitochondrial membrane potential was examined by rhodamine 123 staining. The appearance of green fluorescence in untreated cells which are in live state have higher membrane potential and high uptake of fluorescent dye. Bak tends to decrease membrane potential of mitochondria in A431 cells in concentration-dependent manner as represented in Fig. 3E. The alteration in membrane potential has been originally assumed to be an early process in apoptosis signaling pathway.

3.5. Flow cytometric analysis

3.5.1. Assessment of mitochondrial membrane potential

Rhodamine 123 is a fluorescent probe was utilized in this study to examine the changes in membrane potential of mitochondria and it is a key method to determine process of cell death. In the assay, M1 represents decrease in membrane potential, whereas M2 showed the intact cells percentage. The outcomes of procedure revealed that varied concentrations IC_{30} (2.10 μM/ml), IC_{50} (9.06 μM/ml), and IC_{70} (38.88 μM/ml) of Bak treated A431 cells showed 58.2%, 73.9% and 83.4% increase in the depolarization of mitochondrial membrane potential in A431 cells with respect to control cells 47.9% as shown in Fig. 4A; Fig. S5.

3.5.2. Analysis of ROS (Reactive oxygen species)

The accumulation of ROS possesses a significant role in inducing cell death and depolarization of the mitochondrial membrane. During the experiment, DCFH-DA (2′, 7′-dichlorofluorescein diacetate) stain was used to measure the level of accumulated ROS. DCFH-DA, is cell membrane permeable and chemiluminescent probe that simply passes and deacetylated by enzyme esterases into DCFH non-fluorescent probe (Eruslanov and Kusmartsev, 2010). On quenching, reactive peroxidases oxidized DCFH and H_2O_2 into fluorescent 2,7- dichlorofluorescein (DCF) that was analyzed by flow cytometer. The fluorescence intensity is directly proportional to percentage of generated ROS in cell cytoplasm. In the present study, M1 represents live cells (ROS negative), whereas M2 represents accumulated ROS level (ROS positive). On treatment with varying concentrations (2.10 μM/ml, 9.06 μM/ml and 38.88 μM/ml) of Bak, a notable increase in the generation of ROS (M2) was observed in cells by 27.2%, 39.0% and 45.2% as compared to control 23.6% respectively in a dose-dependent manner (Fig. 4B; Fig. S6)0.*3.5.3. Cell Cycle phase distribution*.

Cell cycle analysis by flow cytometry is useful to differentiate phases of cell cycle and fragmentation of DNA during cell death. In this study, the treatment of Bak reveals the gradual increase in the percentage of cells at phases G_0/G_1 whereas decrease in population of cells at S and G_2/M phases of cell cycle in a dose-dependent way. The varying doses (2.10 μM/ml, 9.06 μM/ml and 38.88 μM/ml) of Bak showed an increment in population of cells at G_0/G_1 phases of the cell cycle by 68.7%, 77.0%, 81.4% respectively in A431 cells with respect to untreated control 55.3% as shown in Fig. 4C; Fig. S7.

3.5.3. Apoptosis assay using Annexin V-FITC

A431 cells undergoes programmed cell death or necrotic mode on Bak treatment, Annexin V-FITC and PI stain was utilized to perform flow cytometric technique. In mechanism of apoptosis, phosphatidylserine flip towards external surface of plasma membrane that normally presented towards inner side. Annexin V-FITC and PI stain useful to examine percentage of cells in different phases of apoptosis. Our outcomes of the experiment showed that on Bak treatment, a significant decrease in A431 cells via apoptotic mode in a concentration-dependent manner. Bak induces 8.1% to 34.4% increase early apoptosis in cells with respect to the control of 1.8%. Moreover, percentage of enhance in late apoptotic cell population was 0.7% to 7.0% on Bak treatment. Total population percentage of apoptotic cells was 0.9% to 7.2% with respect to untreated control value of 0.2% (Fig. 4D). The histograms show the decreased percentage of live cells population in a concentration-dependent way compared to control (Fig. S8).

3.6. RT-qPCR analysis

The effect of Bak was determined on the expression of TLR 9, IFN β, IL 23, JAK 3 and STAT 3 by qRT-PCR. Using comparative threshold cycle method (ΔΔCT), each gene expression was calculated. β-actin was taken as control and Ct value of each was neutralized by Ct value of β-actin. All genes expression were represented as $2^{-\Delta\Delta Ct} \pm SE$.

Results represents expression of these genes was found to be decreased after the treatment with different concentrations IC_{30} (2.10 μM/ml), IC_{50} (9.06 μM/ml) and IC_{70} (38.88 μM/ml of Bak as compared to untreated control in squamous skin carcinoma A431 cells as shown in Fig. 5. The result showed decrease in expression of inflammatory markers on treatment with Bak induces cell death in A431 cells through an inflammation-mediated molecular signaling network.

3.7. Molecular docking

The molecular docking studies were studied to reveal molecular interactions of JAK3 kinase with Bak. X-ray crystallographic structure of JAK3 kinase in complex with its inhibitor 9YV (PDB entry: 5 W86; Resolution: 2.61 Å) was employed (https://www.rcsb.org/structure/5w86) for this purpose. The precision of docking protocol was confirmed by docking co-crystallized ligand 9YV into its binding site. The database was capable to produce best-fit conformation of 9YV with root mean square deviation (RMSD) value of 0.7138, represents the reliability of docking. Afterwards, docking of Bak into 9YV binding site and best pose with −10.1939 score was taken for discussion (Fig. 6).

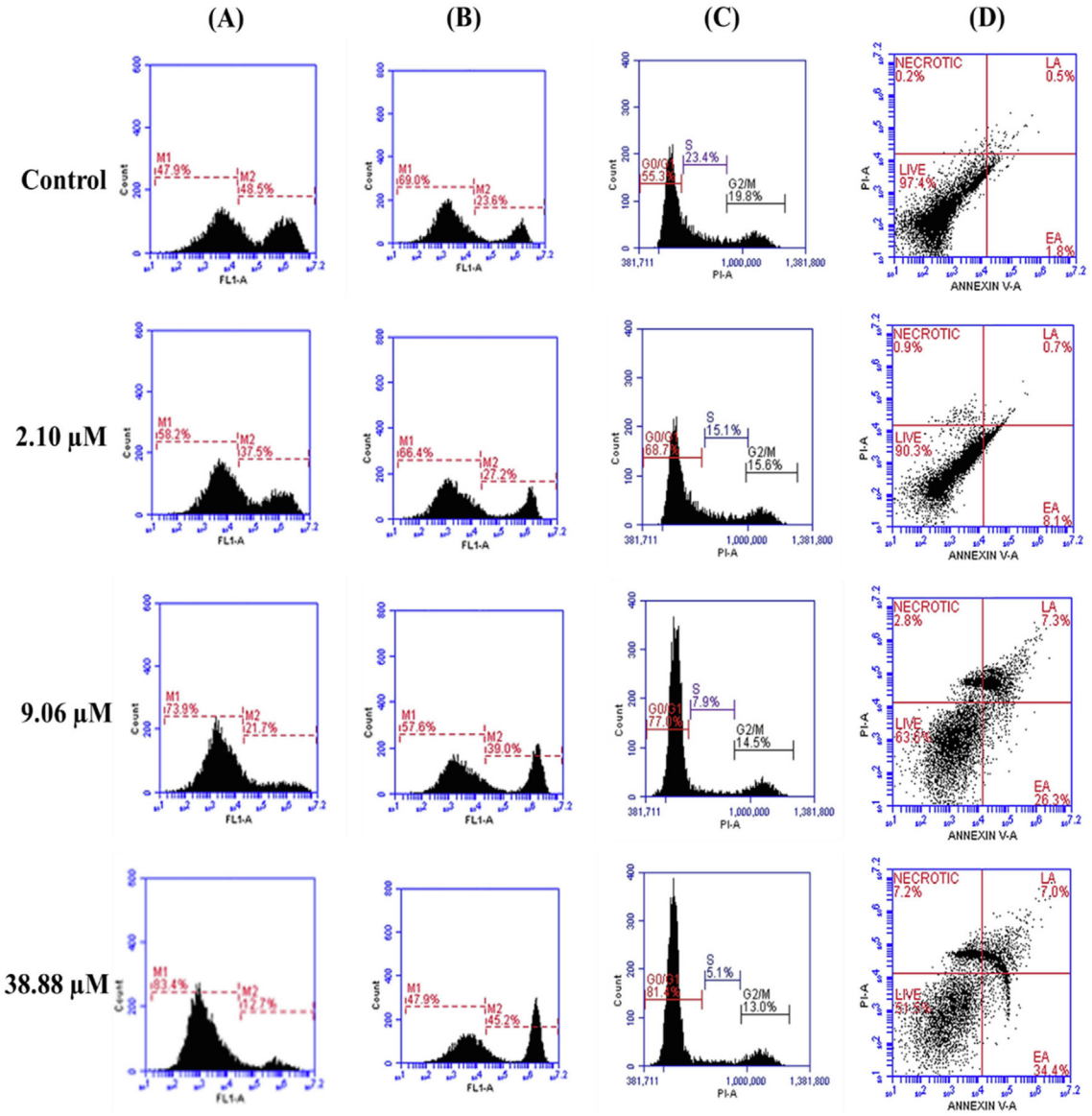

Fig. 4. **(A)** The disruption of mitochondrial membrane potential ($\Delta\Psi m$) in A431 cells on treatment with bakuchiol via using Rhodamine-123 staining. **(B)** The accumulation of intracellular ROS in A431 cells were detected using DCFH-DA staining **(C)** The induction of cell cycle arrest as detected by using PI staining. **(D)** Detection of apoptosis and necrosis using Annexin V-FITC and PI dual staining, results are expressed as total percentages of cells present in four different quadrants: Live cells (Annexin V and PI negative), early apoptosis (EA = Annexin V- positive, PI negative), late apoptosis (LA = Annexin V-positive, PI positive) necrosis (Annexin V-negative, PI positive).

4. Discussion

Over the last few decades, an increasing incidence of NMSC has been observed which may be linked to several risk factors. Although great achievements have been acquired during early diagnosis, but still not much success has been achieved in decreasing NMSC morbidity and death. Surgery and radiation therapies are the major treatment modalities but these have been associated with severe side effects. Literature surveys indicate that the natural compounds can prove to be safe and effective to inhibit the progression of cancer cells via induction of apoptosis and anti-inflammatory response. The number of botanicals have the tendency to alter the molecular signaling cascade because of their variable biological properties like anti-metastatic, anti-inflammatory, antioxidant, anti-proliferative and pro-apoptotic (Gali-Muhtasib et al., 2015). These natural constituents precisely block the progression of cancer by restoring damage of DNA and decreasing inflammation. The epidemiological association within cancer and inflammation has been well recognized. At the position of chronic inflammation, many types of cancer arise and initiate the production of inflammatory markers in tumors. So, use of drugs with anti-inflammatory potential is one of the targeted approaches to reducing the occurrence of human tumors (Fukuda et al., 2010).

In our present study, we focused on bakuchiol (Bak), an isolated meroterpene from plant *Psoralea corylifolia,* widely used herb against various skin disorders including cancer. We examined the anti-cancer potential of bakuchiol against human squamous cell-derived A431 cancerous cell line as well as normal fibroblast L929 cell line. The outcomes of the experiment revealed that Bak showed anticancer effect and proved to be an effective chemopreventive/chemotherapeutic constituent for cancer especially cancer. However, the effect of Bak on skin cancer and associated mechanism of action has not been fully explored. So, in the present research, we investigated the molecular mechanism of anti-cancer potential of Bak against A431 cell line by evaluating its effects on apoptosis and by targeting its effects on the molecular

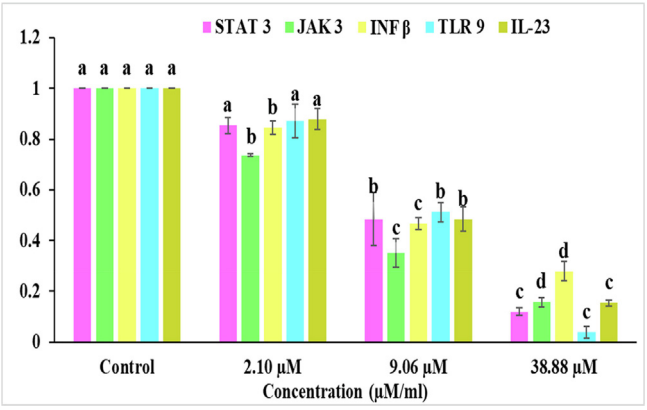

Fig. 5. Bakuchiol treatment significantly downregulates the gene expression of STAT 3, JAK 3, INF β, TLR 9 and IL-23 in A431 cell line. The values are presented as Mean ± SE of three determinations, and data labels with small letters (a, b, c and d) indicates significant difference among them at $p \leq 0.05$ level of significance respective to the control.

markers viz. TLR 9, IL 23, IFN β, JAK 3 and STAT 3 of inflammatory pathways to attenuate skin carcinogenesis.

Our *in vitro* data showed that Bak inhibited the growth of human squamous carcinoma A431 cell line with IC_{30} value of 2.10 µM/ml, IC_{50} value of 9.06 µM/ml and IC_{70} value of 38.88 µM/ml as compared to normal cell line with IC_{50} value of 75.12 µM/ml. A study reported by Kamatham et al., (2015) showed that the isolated Gallic acid (GA) and its derivative methyl gallate (MG) from the methanolic seed extract of *Givotia rottleriformis* exhibited growth inhibitory effect on human epidermoid carcinoma A431 cells. Another study showed that bakuchiol effectively inhibited the growth of human lung adenocarcinoma A549 cell line as compared to resveratrol and showed anti-tumor properties (Chen et al., 2010).

Evaluation of apoptosis induction in A431 cell line on treatment with Bak, showed the morphological alterations including cell shrinkage, fragmentation and condensation of chromatin, membrane blebbing as analyzed by using SEM microscopy, AO/EtBr, Hoescht 33,342 and Rhodamine 123 staining (Fluorescence microscopy). The outcomes indicated that Bak induced cell apoptosis in these cells. This is consistent with a study conducted by Wang et al., (2011) that revealed that psoralen and isopsoralen induced cell death in Human oral carcinoma (KB) cells. They showed membrane shrinkage of cell, condensation of chromatin and rough appearance of nuclear architecture with respect to control which exhibits normal morphology. Isowighteone, an isolated compound of *Psoralea corylifolia* induced apoptosis in mammalian cells (H4IIE, Hct116, C6) characterized by the formation of apoptotic bodies with clearly fragmented and condensed nuclei along with visible membrane blebbing(Limper et al., 2013).

To date, various research reports reveal that enhanced oxidative stress because of accumulation of ROS (reactive oxygen species) alters metabolic activities which results in the initiation of different types of cancer. The increase in cellular ROS level leads to various responses ranging from an enhancement in proliferation of cells, senescence, cell death and finally necrosis (Afriet al., 2004). Kong and Lillehei, (1998) proposed that various chemotherapeutic agents showed apoptosis-inducing potential via accumulating ROS in tumor cells. ROS accumulating constituents can be considered as a therapeutic approach to induce programmed cell death in cancer cells. Our study demonstrated that after the treatment with increasing concentrations (IC_{30}; 2.10 µM/ml, IC_{50}; 9.06 µM/ml and IC_{70}; 38.88 µM/ml) of Bak, there was an increase in the disruption of membrane potential of mitochondria, increase in level of ROS, inhibits progression of cell cycle at phase G_0/G_1 and enhance the percentage of apoptotic cell population. A study reported by Li et al., (2017) showed that bakuchiol induced cell death and decreased membrane potential of mitochondrial in breast cancer stem cells. Bavachinin is another potent flavanone component of *P. corylifolia* induced cell cycle arrest at G_2/M phase via modulating

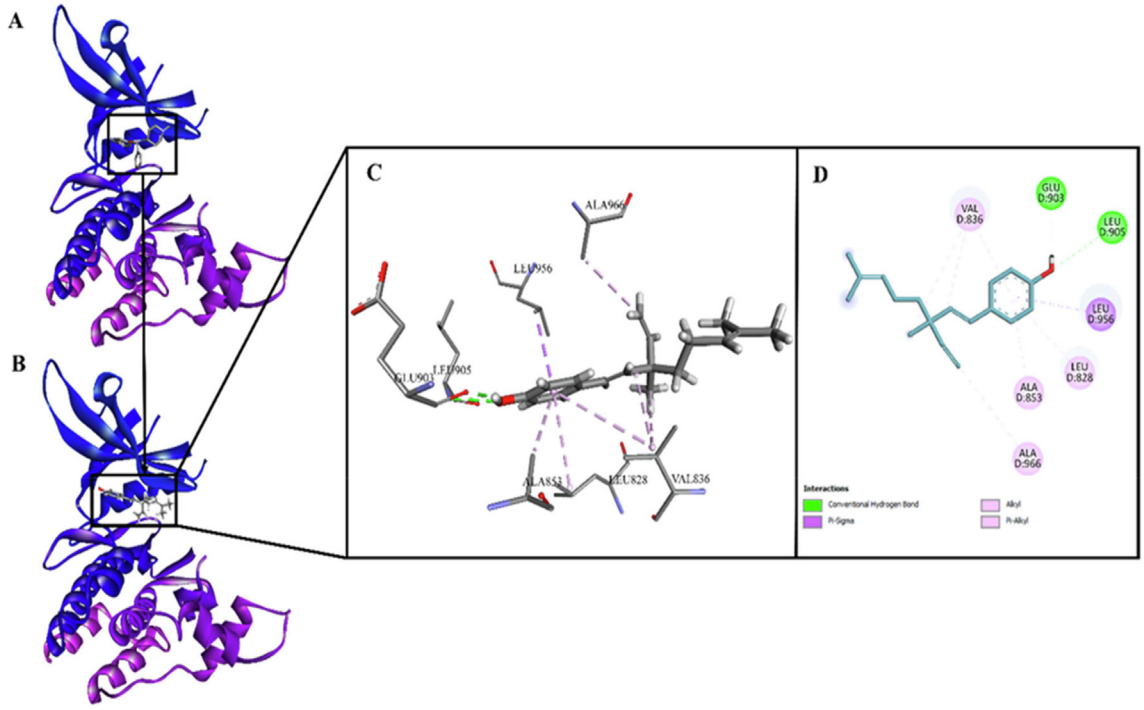

Fig. 6. (A). JAK3 kinase in complex with its inhibitor 9YV (PDB entry: 5 W86; Resolution: 2.61 Å); **(B).** Bakuchiol docked on binding site of JAK3 kinase; **(C).** 3D view of interactions of bakuchiol with residues of binding site of JAK3 kinase; **(D).** 2D view of interactions of bakuchiol with residues of binding site of JAK3 kinase.

p38 MAPK-dependent p21Waf1/Cip1-mediated pathway in non-small cell lung cancer (NSCLC) cells (Pai et al., 2021). According to Madrid et al., (2015), Bakuchiol isolated from the plant *Psoralea glandulosa* possesses cytotoxicity towards melanoma cells by triggering the process of apoptosis by decreasing the mitochondrial membrane potential ($\Delta\Psi m$), inducing caspase 9/3 activation and p53, upregulation of Bax as well as downregulation of Bcl-2 expression.

The major reason for skin carcinogenesis is UVB radiations which penetrate the epidermis and can induce variable acute and chronic ill-effects such as photoaging of the skin, inflammation, immunosuppression and direct DNA damage. Additionally, it can induce DNA damage indirectly by generating free radicals and oxidative stress. Another major factor that is responsible for the development and progression of skin cancer is inflammation (Singh et al., 2014). In addition to this, neutrophilic infiltration induces the production of ROS and RNS, which can cause chromatin damage and promote DNA mutagenesis or activate an intercellular signal transduction cascade that leads to inflammation and tumor formation (Kruk and Duchnik, 2014).

One of the important pathways involved in the development of skin carcinogenesis is Janus kinase/signal transducers and activators of the transcription (JAK/STAT) pathway (Pan et al., 2020). The JAK/STAT pathway induces the release of different inflammatory markers including cytokines, chemokines growth factors and various other membrane receptors. Extreme secretion of inflammatory markers results in chronic inflammation, results enhance initiation of carcinogenesis. So, regulating inflammation process of the skin towards solar radiation might be a useful mechanism to suppressing risk of skin cancer. In present study, we observed level of various markers that may be directly or indirectly interact in process of inflammation. Our results showed that after the treatment of Bak, there is decrease in the expression level of Toll-like receptor 9 (TLR 9), Interferon-β (IFN-β), Interleukin 23 (IL 23), Janus kinases (JAK 3) and signal transducer and activator of transcription proteins (STAT 3). In a reported study, it was found that bavachin, bakuchiol, bavachinin, corylin, corylifol A, neobavaisoflavone and isobavachalcone block the activity of IL-6-induced STAT3 activation that helps to cure inflammatory diseases (Lee et al., 2012). JAK/STAT pathway enrolls an essential route in the modulation of various responses. The major proteins imparts in JAK/STAT signaling, involves JAK and STAT and cell-surface receptors. In literature, various bioactive phyto compounds have been reported for their potential to inhibit the JAK/STAT pathway by variable mechanisms. One of the examples is bavachin, isolated from the plant *Psoralea corylifolia* induced apoptosis in various myeloma cell lines by inhibiting the activation and phosphorylation of STAT 3 (Takeda et al., 2018). In addition, Yang et al., (2011) reported that Psoralidin decreased inflammation in human normal lung-fibroblasts and mice, by ionizing radiation via regulating the expression of pro-inflammatory cytokines. Several agonists of TLR have been reported to cure skin cancer such as Imidazoquinolines (TLR7 and −8 agonists) and CpG oligodeoxynucleotides (ODNs) (TLR9 agonists) etc. After binding to the ligands, dimerization of TLRs undergoes a structural change which further activates the downstream signaling cascade. This inturn leads to the release of numerous inflammatory factors like IFN α, IL 1, 6 and 8, tumor necrosis factor α (TNF-α) and IFN β (Coati et al., 2016). So, the therapeutic aim is to decrease the inflammatory web in neoplastic tissues by downregulating the level of pro-inflammatory

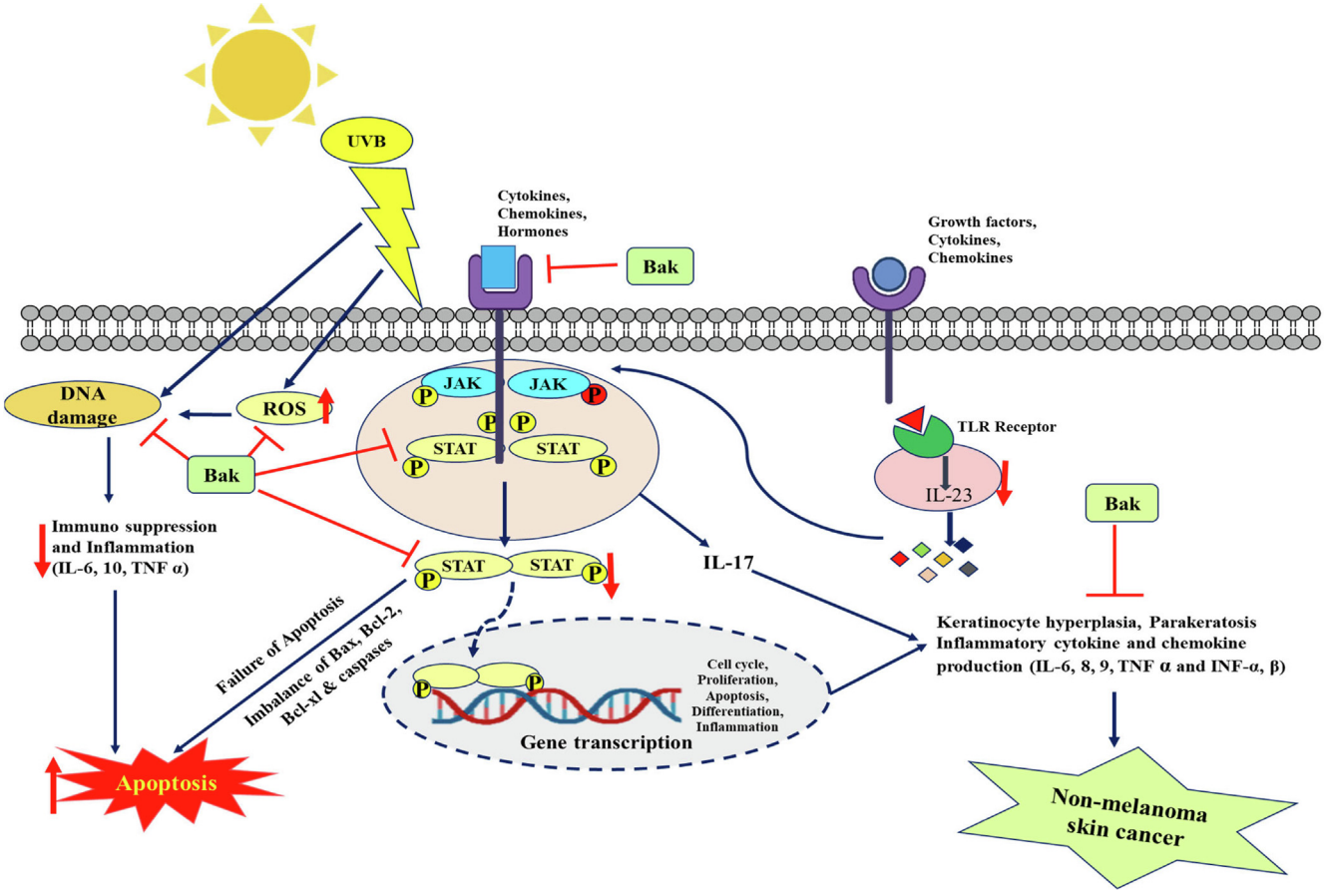

Fig. 7. Schematic diagram of apoptosis inducing potential of bakuchiol as well as reduced inflammation by targeting inflammatory markers in skin squamous cell carcinoma A431 cells.

markers/cytokines and upregulating expression level of anti-inflammatory factors.

To elucidate the mechanism that how Bak blocks the activity of JAK 3 further, we conducted a computational modeling study. The binding pattern of Bak within the adherent position discloses that Bak is best fit in the cavity which is maintained/neutralized via different electrostatic interactions. The important interactions of Bak along JAK3 kinase include π-σ, π-alkyl, alkyl and conventional hydrogen bond interaction. The aromatic ring of Bak is well-positioned in the cavity formed by Leu956, Leu905, Glu903, Ala853, Leu828 and Val836. The Hydroxyl group on aromatic ring of Bak is making conventional hydrogen bond interactions with Leu905 (H-bond acceptor; d = 2.73 Å) and Glu903 (H-bond acceptor; d = 2.00 Å). Aromatic ring is making π-σ type interaction with Leu956 while π-alkyl interactions with Ala853, Leu828 and Val836, depicting the stronghold of the aromatic ring in the binding site. Alkyl chain of Bak is found to interact with Ala966 and Val836 through alkyl interactions. The overall study proposed that Bak is an ideal scaffold that can complete the pharmacophoric need for inhibition of JAK3 kinase.

Overall, our study demonstrates that Bak isolated from the *Psoralea corylifolia* plant has a notable antiproliferative and anti-inflammatory activity by inducing apoptosis and regulating the levels of inflammatory markers such as TLR 9, IFN-β, IL 23, JAK 3 and STAT 3 which are involved in the process of skin carcinogenesis (Fig. 7).

5. Conclusion

Chronic inflammation appears to be one of the major hallmarks of solar UVR and agent-mediated skin cancers. A variety of cytokines, chemokines and growth receptors are identified to play a significant role in skin inflammation as well as carcinogenesis. Therefore, understanding the role of inflammation and apoptosis in the initiation, promotion and progression of skin cancer, an alternative and safe therapeutic approach with deep mechanistic insight is required. The present study demonstrated that Bak isolated from *Psoralea corylifolia* exhibited strong cytotoxic potential towards A431 squamous cell carcinoma cells via enhancing cell death and reducing inflammation by targeting TLR 9, IFN-β, IL 23, JAK 3 and STAT 3 gene markers. On the treatment of Bak, the expression level of targeted inflammatory markers became down-regulated and also caused cell death via initiating the process of apoptosis as analyzed by microscopic and flow cytometric studies. A computational modeling study also confirmed that Bak has an ideal scaffold that can complete the pharmacophoric need for JAK3 kinase inhibition. The overall findings of the present research provide evidence for anticancer, apoptosis-inducing and anti-inflammatory potential of Bak and depict helpful information for future studies that will lead to its application in blocking the progression and development of skin cancer by targeting inflammatory pathways.

Declaration of Competing Interest

The authors declare that they have no known competing financial interests or personal relationships that could have appeared to influence the work reported in this paper.

Acknowledgments

The authors are thankful to the Council of Scientific and Industrial Research (CSIR), New Delhi India for providing financial assistance. The researchers would like to acknowledge the Deanship of Scientific Research, Taif University, Saudi Arabia for funding this work. We would like to acknowledge Dr. Hardeep Tuli and Prof.. Steve Harakeh for their kind help during research. We like to acknowledge DST-PURSE, DST-FIST programmer, RUSA 2.0, UGC, New Delhi for the instrumentation facility provided under UGC-DRS V, CPEPA and UPE program and Centre of Emerging Life Sciences, Guru Nanak Dev University, Amritsar (India) for providing the required support and facilities.

Appendix A. Supplementary data

Fig. S1: ^{1}H NMR of the Bak from *PcH* of *P. corylifolia*, Fig. S2: ^{13}C NMR of the Bak from *PcH* of *P. corylifolia*, Fig. S3: FT-IR (Fourier-transform infrared) spectrum of the Bak from *PcH* of *P. corylifolia*, Fig. S4: The HRMS (High-Resonance Mass Spectroscopy) chromatogram of the Bak from *PcH* of *P. corylifolia*, Fig. S5: Histograms showing disruption of mitochondrial membrane potential ($\Delta\Psi$m) and intact cell population after treatment with IC_{30} (2.10 μM/ml), IC_{50} (9.06 μM/ml), IC_{70} (38.88 μM/ml) of bakuchiol isolated from *P. corylifolia* using flow cytometer. Experiments were repeated at least three times. Data are presented as Mean ± SE. Data labels with different letters (a, b, c and d) represent significant difference among them at the level of significance $p \leq 0.05$., Fig. S6: Histograms showing accumulation of reactive oxygen species and intact cell population after treatment with IC_{30} (2.10 μM/ml), IC_{50} (9.06 μM/ml), IC_{70} (38.88 μM/ml) of bakuchiol isolated from *P. corylifolia* using flow cytometer. Experiments were repeated at least three times. Data are presented as Mean ± SE. Data labels with different letters (a, b, c and d) represent significant difference among them at the level of significance $p \leq 0.05$., Fig. S7: Histograms showing distribution of cells at different phases G_0/G_1, S and G2/M of cell cycle after treatment with IC_{30} (2.10 μM/ml), IC_{50} (9.06 μM/ml), IC_{70} (38.88 μM/ml) of bakuchiol isolated from *P. corylifolia* using flow cytometer. Experiments were repeated at least three times. Data are presented as Mean ± SE. Data labels with different letters (a, b, c and d) represent significant difference among them at the level of significance $p \leq 0.05$, Fig. S8: Histograms showing percentage of Live, EA, LA and necrotic cells using Annexin V-FITC double staining using flow cytometry after treatment with IC_{30} (2.10 μM/ml), IC_{50} (9.06 μM/ml), IC_{70} (38.88 μM/ml) of bakuchiol isolated from *P. corylifolia* respectively. Experiments were repeated at least three times. Data are presented as Mean ± SE. Data labels with different letters (a, b, c and d) represent significant difference among them at the level of significance $p \leq 0.05$.

Supplementary data to this article can be found online at https://doi.org/10.1016/j.jksus.2023.102716.

References

Afri, M., Frimer, A.A., Cohen, Y., 2004. Active oxygen chemistry within the liposomal bilayer: part IV: locating 2′, 7′-dichlorofluorescein (DCF), 2′, 7′-dichlorodihydrofluorescein (DCFH) and 2′, 7′-dichlorodihydrofluorescein diacetate (DCFH-DA) in the lipid bilayer. Chem. Phys. Lipids. 131, 123–133. https://doi.org/10.1016/j.chemphyslip.2004.04.006.

Al-Oqail, M.M., Farshori, N.N., Al-Sheddi, E.S., Al-Massarani, S.M., Saquib, Q., Siddiqui, M.A., 2021. Oxidative Stress Mediated Cytotoxicity, Cell Cycle Arrest, and Apoptosis Induced by Rosa damascena in Human Cervical Cancer HeLa Cells. Oxid. Med. Cell. Longev.. 2021, 1–11. https://doi.org/10.1155/2021/6695634.

Barton, V., Armeson, K., Hampras, S., Ferris, L.K., Visvanathan, K., Rollison, D., 2017. Nonmelanoma skin cancer and risk of all-cause and cancer-related mortality: a systematic review. Arch. Dermatol. Res.. 309, 243–251. https://doi.org/10.1007/s00403-017-1724-5.

Bucevičius, J., Lukinavičius, G., Gerasimaitė, R., 2018. The use of Hoechst dyes for DNA staining and beyond. Chemosensors. 6, 18. https://doi.org/10.3390/chemosensors6020018.

Cen, X., Liu, S., Cheng, K., 2018. The role of toll-like receptor in inflammation and tumor immunity. Front. Pharmacol. 9, 878. https://doi.org/10.3389/fphar.2018.00878.

Chamcheu, J.C., Rady, I., Chamcheu, R.C.N., Siddique, A.B., Bloch, M.B., BanangMbeumi, S., 2018. Graviola (Annona muricata) exerts anti-proliferative, anti-clonogenic and pro-apoptotic effects in human non-melanoma skin cancer UW-BCC1 and A431 cells in vitro: involvement of hedgehog signaling. Int. J. Mol. Sci. 19, 1791. https://doi.org/10.3390/ijms19061791.

Chen, Z., Jin, K., Gao, L., Lou, G., Jin, Y., Yu, Y., 2010. Anti-tumor effects of bakuchiol, an analogue of resveratrol, on human lung adenocarcinoma A549 cell line. Eur. J. Pharmacol.. 643, 170–179. https://doi.org/10.1016/j.ejphar.2010.06.025.

Coati, I., Miotto, S., Zanetti, I., Alaibac, M., 2016. Toll-like receptors and cutaneous melanoma. Oncol. Lett.. 12, 3655–3661. https://doi.org/10.3892/ol.2016.5166.

Eruslanov, E., Kusmartsev, S., 2010. Identification of ROS using oxidized DCFDA and flow-cytometry. In Advanced protocols in oxidative stress II. Humana Press, Totowa, NJ. 2010, 57–72. https://doi.org/10.1007/978-1-60761-411-1_4.

Fattahi, S., Ardekani, A.M., Zabihi, E., Abedian, Z., Mostafazadeh, A., Pourbagher, R., 2013. Antioxidant and apoptotic effects of an aqueous extract of Urtica dioica on the MCF-7 human breast cancer cell line. Asian Pac. J. Cancer Prev. 14, 5317–5323. https://doi.org/10.7314/APJCP.2013.14.9.5317.

Fukuda, M., Ehara, M., Suzuki, S., Ohmori, Y., Sakashita, H., 2010. IL-23 promotes growth and proliferation in human squamous cell carcinoma of the oral cavity. Int. J. Oncol.. 36, 1355–1365. https://doi.org/10.3892/ijo_00000620.

Gali-Muhtasib, H., Hmadi, R., Kareh, M., Tohme, R., Darwiche, N., 2015. Cell death mechanisms of plant-derived anticancer drugs: beyond apoptosis. Apoptosis. 20, 1531–1562. https://doi.org/10.1007/s10495-015-1169-2.

Grace Nirmala, J., Evangeline Celsia, S., Swaminathan, A., Narendhirakannan, R.T., Chatterjee, S., 2018. Cytotoxicity and apoptotic cell death induced by Vitis vinifera peel and seed extracts in A431 skin cancer cells. Cytotechnology. 70, 537–554. https://doi.org/10.1007/s10616-017-0125-0.

Jafernik, K., Halina, E., Ercisli, S., Szopa, A., 2021. Characteristics of bakuchiol-the compound with high biological activity and the main source of its acquisition-Cullen corylifolium (L.) Medik. Nat. Prod. Res. 35, 5828–5842. https://doi.org/10.1080/14786419.2020.1837813.

Kamatham, S., Kumar, N., Gudipalli, P., 2015. Isolation and characterization of gallic acid and methyl gallate from the seed coats of Givotiarottleriformis Griff. and their anti-proliferative effect on human epidermoid carcinoma A431 cells. Toxicol. Rep.. 2, 520–529. https://doi.org/10.1016/j.toxrep.2015.03.001.

Khushboo, P.S., Jadhav, V.M., Kadam, V.J., Sathe, N.S., 2010. Psoralea corylifolia Linn.—"Kushtanashini". Pharmacognosy reviews. 4, 69 10.4103%2F0973-7847.65331.

Kong, Q., Lillehei, K.O., 1998. Antioxidant inhibitors for cancertherapy. Med Hypotheses. 51, 405–409. https://doi.org/10.1054/mehy.1999.0982.

Kruk, J., Duchnik, E., 2014. Oxidative stress and skin diseases: possible role of physical activity. Asian Pac. J. Cancer Prev. 15, 561–568. https://doi.org/10.7314/APJCP.2014.15.2.561.

Kumar, A., Kaur, S., Pandit, K., Kaur, V., Thakur, S., Kaur, S., 2021. Onosma bracteata Wall. induces G 0/G 1 arrest and apoptosis in MG-63 human osteosarcoma cells via ROS generation and AKT/GSK3β/cyclin E pathway. Environ. Sci. Pollut. Res. 28, 14983–15004. https://doi.org/10.1007/s11356-020-11466-9.

Lee, C.W., Kim, S.C., Kwak, T.W., Lee, J.R., Jo, M.J., Ahn, Y.T., An, W.G., 2012. Anti-inflammatory effects of bangpungtongsung-san, a traditional herbal prescription. Evid. Based Complement. Alternat. Med.. 2012, 1–13.

Leiter, U., Garbe, C., 2008. Epidemiology of melanoma and nonmelanoma skin cancer—the role of sunlight. Sunlight, vitamin D and skin cancer. 2008, 89–103. https://doi.org/10.1007/978-0-387-77574-6_8.

Li, L., Liu, C.C., Chen, X., Xu, S., et al., 2017. Mechanistic study of bakuchiol-induced anti-breast cancer stem cell and in vivo anti-metastasis effects. Frontiers in Pharmacology. 8, 746. https://doi.org/10.3389/fphar.2017.00746.

Limper, C., Wang, Y., Ruhl, S., Wang, Z., Lou, Y., Totzke, F., 2013. Compounds isolated from Psoralea corylifolia seeds inhibit protein kinase activity and induce apoptotic cell death in mammalian cells. J. Pharm. Pharmacol. 65, 1393–1408. https://doi.org/10.1111/jphp.12107.

Madrid, A., Cardile, V., González, C., Montenegro, I., Villena, J., Caggia, S., 2015. Psoralea glandulosa as a potential source of anticancer agents for melanoma treatment. Int. J. Mol. Sci.. 16, 7944–7959. https://doi.org/10.3390/ijms16047944.

Pai, J.T., Hsu, M.W., Leu, Y.L., Chang, K.T., Weng, M.S., 2021. Induction of G2/M Cell Cycle Arrest via p38/p21Waf1/Cip1-Dependent Signaling Pathway Activation by Bavachinin in Non-Small-Cell Lung Cancer Cells. Molecules 26, 5161. https://doi.org/10.3390/molecules26175161.

Pan, F., Wang, Q., Li, S., Huang, R., Wang, X., Liao, X., 2020. Prognostic value of key genes of the JAK–STAT signaling pathway in patients with cutaneous melanoma. Oncol. Lett. 19, 1928–1946. https://doi.org/10.3892/ol.2020.11287.

Panda, S., 2010. Nonmelanoma skin cancer in India: Current scenario. Indian J. Dermatol. 55, 373 10.4103%2F0019-5154.74551.

Ramasamy, S.P., Rajendran, A., Pallikondaperumal, M., Sundararajan, P., Husain, F. M., Khan, A., 2022. Broad-Spectrum Antimicrobial, Antioxidant, and Anticancer Studies of Leaf Extract of Simarouba glauca DC In Vitro. Antibiotics. 11, 59. https://doi.org/10.3390/antibiotics11010059.

Singh, M., Suman, S., Shukla, Y., 2014. New enlightenment of skin cancer chemoprevention through phytochemicals: in vitro and in vivo studies and the underlying mechanisms. BioMed research international. 2014, 1–14. https://doi.org/10.1155/2014/243452.

Takeda, T., Tsubaki, M., Tomonari, Y., Kawashima, K., Itoh, T., Imano, M., 2018. Bavachin induces the apoptosis of multiple myeloma cell lines by inhibiting the activation of nuclear factor kappa B and signal transducer and activator of transcription 3. Biomed. Pharmacother. 100, 486–494. https://doi.org/10.1016/j.biopha.2018.02.019.

Tian, Q., Zang, Y.H., 2015. Antiproliferative and apoptotic effects of the ethanolic herbal extract of Achillea falcata in human cervical cancer cells are mediated via cell cycle arrest and mitochondrial membrane potential loss. J BUON. 20, 1487–1496.

Vallée, A., Lecarpentier, Y., 2018. Crosstalk between peroxisome proliferator-activated receptor gamma and the canonical WNT/β-catenin pathway in chronic inflammation and oxidative stress during carcinogenesis. Front. Immunol.. 9, 745. https://doi.org/10.3389/fimmu.2018.00745.

Vijaybabu, K., Punnagai, K., 2019. In-vitro anti-proliferative effects of ethanolic extract of vanilla planifolia leaf extract against A431 human epidermoid carcinoma cells. Biomedical and Pharmacology Journal. 12, 1141–1146 10.13005/bpj/1742.

Wageesha, N.D.A., Soysa, P., Atthanayake, K., Choudhary, M.I., Ekanayake, M.A., 2017. Traditional poly herbal medicine "Le Pana Guliya" induces apoptosis in HepG2 and HeLa cells but not in CC1 cells: an in vitro assessment. Chem. Cent. J. 11, 1–12. https://doi.org/10.1186/s13065-016-0234-4.

Wang, Y., Hong, C., Zhou, C., Xu, D., Qu, H.B., 2011. Screening antitumor compounds psoralen and isopsoralen from Psoralea corylifolia L. seeds. Evid. Based Complement. Alternat. Med. 2011, 1–7. https://doi.org/10.1093/ecam/nen087.

Xian, D., Lai, R., Song, J., Xiong, X., Zhong, J., 2019. Emerging perspective: role of increased ROS and redox imbalance in skin carcinogenesis. Oxid. Med. Cell. Longev. 2019, 1–12. https://doi.org/10.1155/2019/8127362.

Yadav, N.K., Arya, R.K., Dev, K., Sharma, C., Hossain, Z., Meena, S., 2017. Alcoholic extract of Eclipta alba shows in vitro antioxidant and anticancer activity without exhibiting toxicological effects. Oxid. Med. Cell. Longev. 2017, 1–18. https://doi.org/10.1155/2017/9094641.

Yan, W., Wistuba, I.I., Emmert-Buck, M.R., Erickson, H.S., 2011. Squamous cell carcinoma–similarities and differences among anatomical sites. American journal of cancer research. 1, 275-300. www.ajcr.us /ISSN:2156-6976/ajcr0000023.

Yang, H.J., Youn, H., Seong, K.M., Yun, Y.J., Kim, W., Kim, Y.H., 2011. Psoralidin, a dual inhibitor of COX-2 and 5-LOX, regulates ionizing radiation (IR)-induced pulmonary inflammation. Biochem. Pharmacol.. 82, 524–534. https://doi.org/10.1016/j.bcp.2011.05.027.